



HAL
open science

Diode-pumped SESAM mode-locked Yb:(Y,Gd)AlO₃ laser

Wen-Ze Xue, Zhang-Lang Lin, Huang-Jun Zeng, Ge Zhang, Peixiong Zhang, Zhenqiang Chen, Zhen Li, Valentin Petrov, Pavel Loiko, Xavier Mateos, et al.

► **To cite this version:**

Wen-Ze Xue, Zhang-Lang Lin, Huang-Jun Zeng, Ge Zhang, Peixiong Zhang, et al.. Diode-pumped SESAM mode-locked Yb:(Y,Gd)AlO₃ laser. Optics Express, 2022, 30 (7), pp.11825-11832. 10.1364/OE.455303 . hal-03858708

HAL Id: hal-03858708

<https://hal.science/hal-03858708>





Submitted on 17 Nov 2022

HAL is a multi-disciplinary open access archive for the deposit and dissemination of scientific research documents, whether they are published or not. The documents may come from teaching and research institutions in France or abroad, or from public or private research centers.

L'archive ouverte pluridisciplinaire **HAL**, est destinée au dépôt et à la diffusion de documents scientifiques de niveau recherche, publiés ou non, émanant des établissements d'enseignement et de recherche français ou étrangers, des laboratoires publics ou privés.



Diode-pumped SESAM mode-locked Yb:(Y,Gd)AlO₃ laser

WEN-ZE XUE,¹ ZHANG-LANG LIN,¹ HUANG-JUN ZENG,¹
GE ZHANG,¹ PEIXIONG ZHANG,² ZHENQIANG CHEN,² ZHEN LI,²
VALENTIN PETROV,³  PAVEL LOIKO,⁴ XAVIER MATEOS,⁵ 
HAIFENG LIN,⁶ YONGGUANG ZHAO,⁷  LI WANG,³ 
AND WEIDONG CHEN^{1,3,*} 

¹Fujian Institute of Research on the Structure of Matter, Chinese Academy of Sciences, 350002 Fuzhou, China

²Department of Optoelectronic Engineering, Jinan University, 510632 Guangzhou, China

³Max Born Institute for Nonlinear Optics and Short Pulse Spectroscopy, Max-Born-Str. 2a, 12489 Berlin, Germany

⁴Centre de Recherche sur les Ions, les Matériaux et la Photonique (CIMAP), UMR 6252

CEA-CNRS-ENSICAEN, Université de Caen, 6 Boulevard Maréchal Juin, 14050 Caen Cedex 4, France

⁵Universitat Rovira i Virgili, URV, Física i Cristal·lografia de Materials i Nanomaterials (FiCMA-FiCNA)-Marcel·lí Domingo 1, 43007 Tarragona, Spain

⁶College of Physics and Optoelectronic Engineering, Shenzhen University, 518118 Shenzhen, China

⁷Jiangsu Key Laboratory of Advanced Laser Materials and Devices, Jiangsu Normal University, 221116 Xuzhou, China

*chenweidong@fjirsm.ac.cn

Abstract: We report on the continuous-wave (CW) and mode-locked (ML) laser performance of an Yb³⁺-doped yttrium-gadolinium orthoaluminate crystal, Yb:(Y,Gd)AlO₃. Pumping by a single-transverse-mode fiber-coupled 976 nm InGaAs laser diode, the maximum output power in the CW regime amounted to 429 mW at 1041.8 nm corresponding to a slope efficiency of 51.1% and a continuous wavelength tuning across 84 nm (1011–1095 nm) was achieved. The self-starting ML operation of the Yb:(Y,Gd)AlO₃ laser was stabilized by a semiconductor saturable absorber mirror. Soliton pulses as short as 43 fs were generated at 1052.3 nm with an average output power of 103 mW and a pulse repetition rate of ~70.8 MHz. To the best of our knowledge, our result represents the first report on the passively mode-locked operation of a Yb:(Y,Gd)AlO₃ laser, and the shortest pulse duration ever achieved from any Yb³⁺-doped orthorhombic perovskite aluminate crystals.

© 2022 Optica Publishing Group under the terms of the [Optica Open Access Publishing Agreement](#)

1. Introduction

Rare-earth orthoaluminates with chemical formula REAlO₃ (where RE = Y [1,2], Gd [3], Lu [4,5] or their mixtures [6]) are suitable host materials for doping with laser-active rare-earth ions. These crystals belong to the orthorhombic class possessing a perovskite-type (CaTiO₃) structure (sp. gr. $D_{2h}^{16} - P_{nma}$ or P_{bnm}) [7]. It can be presented as a grid of tilted [AlO₆] octahedra with the RE³⁺ ions occupying the holes between them. There is a single type of rare-earth (RE) sites (Wyckoff: 4c, site symmetry: $C_s = C_{1h}$) with the oxygen coordination representing a distorted octahedron, [REO₈]. One of the well-known representatives of this crystal family is the yttrium orthoaluminate (YAlO₃, shortly YAP or YALO), lattice constants: $a = 5.330 \text{ \AA}$, $b = 7.375 \text{ \AA}$ and $c = 5.180 \text{ \AA}$ (sp. gr. P_{nma}) [7]. It crystallizes in the same binary system (Y₂O₃ – Al₂O₃) as the well-known another and widely used cubic Y₃Al₅O₁₂ (shortly YAG) but the optically biaxial YAlO₃ crystals benefit from their intrinsic birefringence resulting in naturally polarized laser emission and weak depolarization losses.

While the first studies on YAlO_3 focused on Nd^{3+} doping, more recently, it has been proven to serve as an excellent host matrix for other RE dopants such as Yb^{3+} [1,8], Tm^{3+} [2,9] or Ho^{3+} [10]. The dopant ions replace the host-forming Y^{3+} cations in the single type RE sites with VIII-fold oxygen coordination. In particular, the ytterbium (Yb^{3+}) ions benefit from a simple energy-level scheme consisting of just two multiplets (${}^2\text{F}_{7/2}$: ground-state, ${}^2\text{F}_{5/2}$: excited-state) leading to high laser efficiencies and weak heat load (as compared to Nd^{3+} ions) and they can be efficiently pumped by commercially available InGaAs diode lasers emitting at 0.98 μm . Yb^{3+} -doped YAlO_3 has been identified as a promising gain medium for the development of power-scalable, efficient continuous-wave (CW) and femtosecond mode-locked (ML) lasers operating at 1 μm [1,8]. This is due to a combination of good thermo-mechanical and spectroscopic properties of this material [11,12]. The thermal conductivities of 5 at.% Yb^{3+} -doped YAlO_3 are relatively high, $\kappa_a = 7.1$, $\kappa_b = 8.3$ and $\kappa_c = 7.6$ W/mK [13]. $\text{Yb}^{3+}:\text{YAlO}_3$ exhibits: i) intense and strongly polarized emission bands which is a prerequisite for naturally polarized laser emission, ii) broader gain bandwidth as compared to that of $\text{Yb}:\text{YAG}$, and iii) moderate concentration-quenching of luminescence [1]. YAlO_3 crystals can be easily doped with Yb^{3+} ions up to high concentrations (~10 at.%) and they can be grown by the Czochralski (Cz) method.

Kisel *et al.* reported on the first passively ML diode-pumped $\text{Yb}:\text{YAlO}_3$ laser employing a Semiconductor Saturable Absorber Mirror (SESAM) delivering 225 fs pulses at 1041 nm with an average output power of 0.8 W at a pulse repetition rate of 70 MHz [1]. Later, the same group demonstrated power scaling of a similar laser using a special off-axis pumping scheme reaching an output power of 4 W at 1009.7 nm with a reduced pulse duration of 140 fs while in the CW regime, the laser wavelength was continuously tunable across 67 nm (985.6–1052.7 nm) [14]. Recently, Akbari *et al.* reported on a CW diode-pumped $\text{Yb}:\text{YAlO}_3$ laser generating 7.15 W at 1042 nm with a high slope efficiency of 70% [15].

One way to enlarge the emission bandwidth of crystals for achieving shorter pulses in the ML operation regime is to grow engineered “mixed” (solid solution) materials in isostructural series [16], e.g., $\text{Y}_{1-x}\text{Gd}_x\text{AlO}_3$ or shortly (Y,Gd) AlO_3 [17,18]. The absorption and emission bands of Yb^{3+} ions in such crystals exhibit inhomogeneous spectral broadening due to the compositional disorder related to different multi-ligands around the active ions composed of both Y^{3+} and Gd^{3+} cations (ionic radii: 1.019 Å and 1.053 Å, respectively). However, the “mixing material” for Yb^{3+} -doped crystals has often a cost on the thermal conductivity, a trade off between spectral bandwidth (pulse duration) and power is then done [19].

In the present work, we report on the CW and the first passively ML operation of a “mixed” $\text{Yb}:(\text{Y,Gd})\text{AlO}_3$ crystal reaching sub-50 fs pulse durations.

2. Experimental setup

2.1. Crystal growth

A high-quality “mixed” orthoaluminate single-crystal was grown by the conventional Cz method [17]. The raw materials were RE_2O_3 (RE = Gd, Y, Yb) and Al_2O_3 (purity: 5N) taken according to the composition $\text{Y}_{0.85}\text{Gd}_{0.10}\text{Yb}_{0.05}\text{AlO}_3$. The polycrystalline material for the growth charge was synthesized by the solid-state reaction method. For that, the raw materials were weighed in stoichiometric ratios, thoroughly mixed for 48 h for homogeneity, pressed into disks and heated in air at 1360°C for 30 h. The growth was performed using an Iridium crucible in nitrogen atmosphere.

A seed from an [100] oriented undoped (Y,Gd) AlO_3 was used. The rotation speed was 8 - 15 rpm and the pulling rate was 0.8-1.5 mm/h. After the growth was completed, the crystal was slowly cooled down to room temperature at a rate of 5–25 °C/h. The as-grown crystal had dimensions of $\Phi 30 \times 40$ mm³ and a slight yellow coloration, as shown in Fig. 1. To remove it, the crystal was annealed in air.

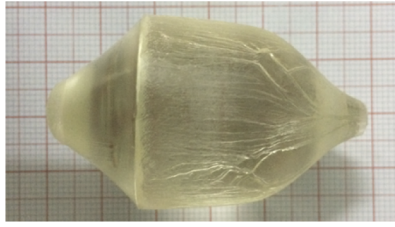


Fig. 1. A photograph of the as-grown 5.65 at.% Yb:(Y,Gd)AlO₃ crystal along the [100] axis.

The actual crystal composition was revealed by the inductively coupled plasma atomic emission spectrometry analysis (ICP-AES) to be Y_{0.8447}Gd_{0.0988}Yb_{0.0565}AlO₃ (5.65 at.% Yb³⁺ doping, the segregation coefficient for Yb³⁺ ions: $K_{Yb} = 1.13$). This doping level is close to the optimum one for Yb³⁺ ions in YAlO₃ as indicated by the analysis of luminescence quenching performed by Boulon *et al.* [1]. The thermal conductivity κ of the compositionally “mixed” Y_{0.8447}Gd_{0.0988}Yb_{0.0565}AlO₃ crystal was estimated to be 6.3 Wm⁻¹K⁻¹ using the analytical model developed by Gaumé *et al.* [20]. According to Aggarwal *et al.*, for undoped YAlO₃, the average κ_0 value is 11.7 Wm⁻¹K⁻¹ at room temperature [13]. Thus, although the introduction of both Yb³⁺ and Gd³⁺ ions induces a certain reduction of thermal conductivity, its value is still high enough to support diode-pumped high-power laser operation.

2.2. Laser set-up

A rectangular laser element was cut from the Yb:(Y,Gd)AlO₃ crystal for light propagation along the crystallographic *c*-axis (*c*-cut) having an aperture of 4(*a*) × 4(*b*) mm² and a thickness of 3 mm (sp. gr. *P_{nma}*). It was double-side polished to laser-grade quality and remained uncoated. This orientation was selected to ensure high pump absorption at ~976 nm. The experimental setup of the Yb:(Y,Gd)AlO₃ laser is shown in Fig. 2.

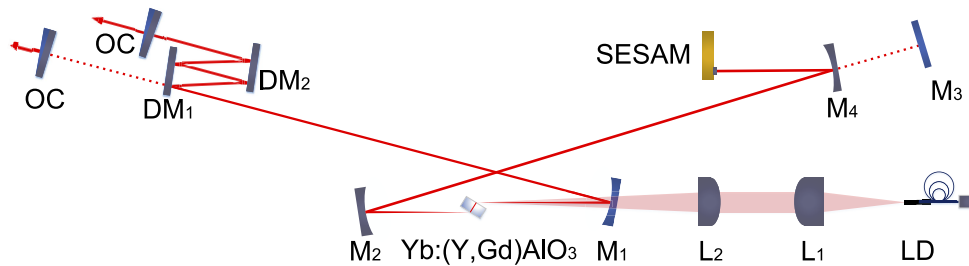


Fig. 2. Experimental setup of the Yb:(Y,Gd)AlO₃ laser. LD: fiber-coupled laser diode at 976 nm; L₁: aspherical lens; L₂: achromatic doublet lens; M₁, M₂ and M₄: concave mirrors (RoC = -100 mm); M₃: flat rear mirror for CW laser operation; DM₁ and DM₂: flat dispersive mirrors; OC: output coupler; SESAM: SEMiconductor Saturable Absorber Mirror.

An X-shaped astigmatically compensated standing-wave resonator was used to evaluate the laser performance both in the CW and ML regimes. The crystal was placed at Brewster’s angle between the two concave folding mirrors M₁ and M₂ (radius of curvature, RoC = -100 mm). It was mounted in a copper holder without active cooling. A single-transverse mode, fiber-coupled InGaAs laser diode delivering a maximum incident power of 1.29 W was employed as a pump source. It had a fiber Bragg grating (FBG) for wavelength locking at 976 nm with a spectral linewidth (full width at half maximum, FWHM) of ~0.2 nm and a nearly diffraction-limited

intensity profile with a beam propagation factor (M^2) of ~ 1.02 . The pump radiation was unpolarized. An aspherical lens L_1 (focal length: $f = 26$ mm) and an achromatic doublet lens L_2 ($f = 100$ mm) were employed to reimaging the pump beam into the laser crystal yielding a beam waist (radius) of $18.9 \mu\text{m} \times 40.4 \mu\text{m}$ in the sagittal and tangential planes, respectively.

In the CW regime, a four-mirror cavity was used. One cavity arm was terminated by a flat rear mirror M_3 and the other arm – by a flat output coupler (OC) having a transmission at the laser wavelength T_{OC} in the range 1% - 10%. The corresponding cavity mode size in the laser crystal was estimated using the ABCD formalism yielding radii of $20.9 \mu\text{m} \times 38.9 \mu\text{m}$ in the sagittal and the tangential planes, respectively. The measured single-pass pump absorption under lasing conditions depended on the transmission of the OC ranging from 76.7% to 81%.

For ML operation, the flat rear mirror M_3 was substituted by a curved mirror M_4 (RoC = -100 mm) for creating a second beam waist on the SESAM with a calculated beam radius of $\sim 39 \mu\text{m}$ to ensure its efficient bleaching. A commercially available SESAM (BATOP, GmbH) with a modulation depth of 0.9%, a relaxation time of ~ 10 ps and a non-saturable loss of $\sim 0.6\%$ at $\sim 1 \mu\text{m}$ was implemented to start and stabilize the ML operation. Two flat dispersive mirrors (DMs) were introduced in the other cavity arm with the same negative group delay dispersion (GDD) per bounce: $DM_1 = DM_2 = -250 \text{ fs}^2$ to compensate the material dispersion inside the resonator and to balance the self-phase modulation (SPM) induced by the Kerr nonlinearity of the crystal for soliton pulse reshaping. The cavity length of the ML laser was 2.12 m which corresponded to a pulse repetition rate of ~ 70.8 MHz.

3. Continuous-wave laser operation

In the CW regime, the laser generated a maximum output power of 429 mW at 1041.8 nm for an absorbed pump power of 1.04 W with a laser threshold of 184 mW, which corresponded to a slope efficiency of 51.1% for $T_{OC} = 4.5\%$, see Fig. 3(a). The highest slope efficiency of 52.0% was achieved with the highest T_{OC} of 10% for an output power of 401 mW at an absorbed power of 1.03 W. The laser threshold gradually increased with the transmission of the OC, from 117 mW ($T_{OC} = 1\%$) to 255 mW ($T_{OC} = 10\%$). The laser wavelength experienced a monotonic blue-shift with T_{OC} in the range of 1037.1–1055.1 nm, as shown in Fig. 3(b). This behavior is typical for quasi-three-level Yb^{3+} lasers with inherent reabsorption at the laser wavelength. The laser emission was linearly polarized ($E \parallel b$).

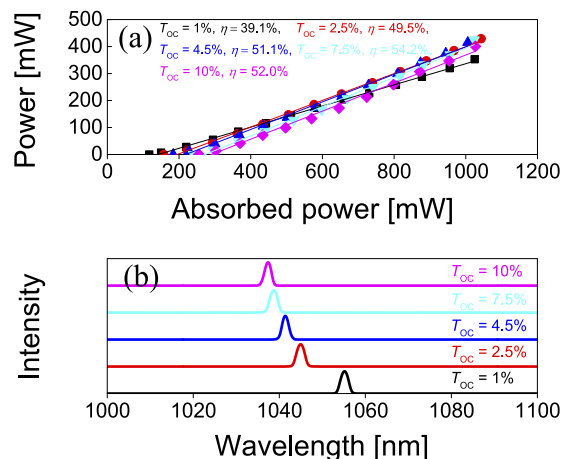


Fig. 3. CW diode-pumped $\text{Yb}:(\text{Y,Gd})\text{AlO}_3$ laser: (a) Input-output dependences for different OCs, η – slope efficiency; (b) Typical spectra of laser emission, $E \parallel b$.

The Caird analysis was applied by fitting the measured laser slope efficiencies as a function of the output coupler reflectivity, $R_{OC} = 1 - T_{OC}$ [21]. The total round-trip cavity losses δ (reabsorption losses excluded), as well as the intrinsic slope efficiency η_0 (accounting for the mode-matching and the quantum efficiencies) were estimated yielding $\eta_0 = 59.4\%$ and $\delta = 0.4\%$, as shown in Fig. 4(a). The low value of δ is an evidence of the good optical quality of the laser crystal (despite being a solid-solution) and the optimized resonator alignment.

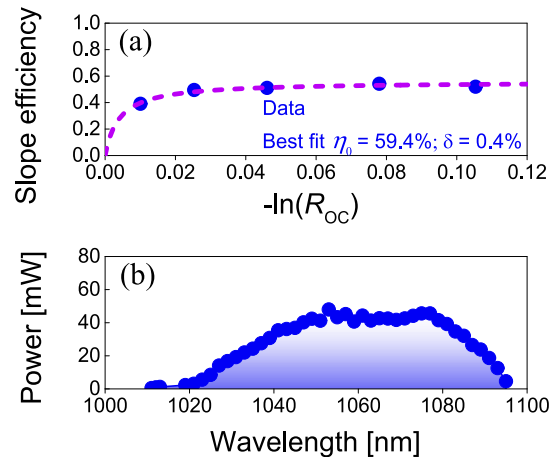


Fig. 4. CW diode-pumped Yb:(Y,Gd)AlO₃ laser: (a) Caird analysis: slope efficiency vs $R_{OC} = 1 - T_{OC}$; (b) Tuning curve obtained with a Lyot filter and $T_{OC} = 0.4\%$ OC. The laser polarization is $\mathbf{E} \parallel \mathbf{b}$.

The wavelength tunability of the Yb:(Y,Gd)AlO₃ laser was investigated by inserting a 2-mm thick quartz plate as a Lyot filter close to the OC ($T_{OC} = 0.4\%$) at an incident pump power of 648 mW. The laser wavelength was continuously tunable between 1011 and 1095 nm in the CW regime, i.e., across 84 nm at the zero-level, Fig. 4(b), which is broader than in the previous work with Yb:YAlO₃ [14].

4. Mode-locked laser operation

Stable and self-starting ML operation was readily obtained by implementing the SESAM and two flat DMs (DM₁ – DM₂) which provided a total round-trip negative GDD of -2000 fs^2 , see Fig. 2. The optimized ML operation of the Yb:(Y,Gd)AlO₃ laser was achieved using a 1.6% OC. Figure 5 shows the characterization of the shortest pulses generated from the ML laser.

Assuming a sech^2 -shaped spectral intensity profile, an emission bandwidth (FWHM) of 29 nm was obtained at a central wavelength of 1052.3 nm, see Fig. 5(a). The observed satellite peak around 1.1 μm originated from the unmanageable intracavity GDD at the long-wave spectral wing and the non-optimized spectral reflectivity of the cavity mirrors. This phenomenon has already been observed in Yb:CALGO [22], and already explained by F. Druon and al. [23]. This could be improved by properly managing the total intracavity GDD over the full spectral bandwidth of the ML laser. The recorded autocorrelation trace could be almost perfectly fitted with a sech^2 -shaped temporal intensity profile, resulting in an estimated pulse duration of 43 fs (FWHM), see Fig. 5(b). The inset in Fig. 5(b) shows an autocorrelation trace on a longer time span of 50 ps revealing single-pulse mode-locking without multiple pulse instabilities. The almost perfectly sech^2 -shaped spectral and temporal intensity profiles indicated soliton-like ML operation. The corresponding time-bandwidth product (TBP) amounted to 0.338 which was slightly above the Fourier-transform-limit (0.315). In these conditions, the maximum average

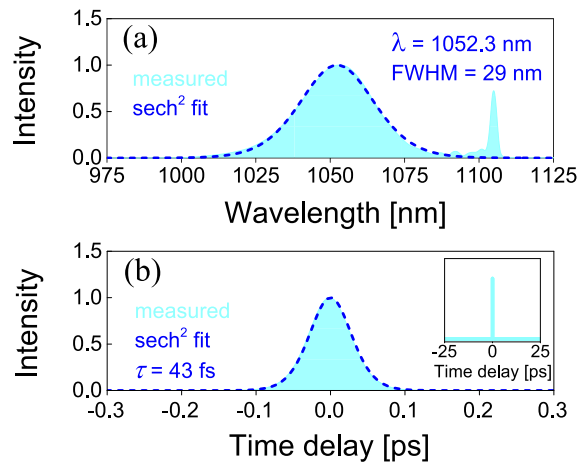


Fig. 5. SESAM ML Yb:(Gd,Y)AlO₃ laser with $T_{\text{OC}} = 1.6\%$. (a) Optical spectrum and (b) SHG-based intensity autocorrelation trace. *Inset:* autocorrelation trace on a time span of 50 ps.

output power amounted to 103 mW at an absorbed pump power of 985 mW, which corresponded to a peak power of 29.8 kW.

The far-field beam profiles both in the CW and the ML regimes were recorded using an IR camera which was placed at 1.2 m from the OC to confirm the dominating ML mechanism, as shown in Fig. 6. The laser beam had a diameter of $1.68 \times 1.69 \text{ mm}^2$ in the CW regime, Fig. 6(a). When mode-locking was initiated by the SESAM, the almost unchanged beam diameter of $1.67 \times 1.68 \text{ mm}^2$ was observed when switching from the CW to ML operation. It was not possible to achieve mode locking when the SESAM was replaced by a dielectric mirror. These observations indicate that the dominant mode-locking mechanism was soliton pulse shaping stabilized by the SESAM without Kerr-lens mode-locking.

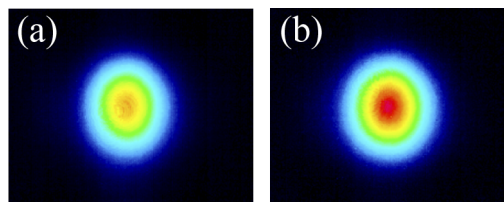


Fig. 6. Measured far-field beam profiles of the Yb:(Y,Gd)AlO₃ laser: (a) CW and (b) ML regimes of operation.

The radio frequency (RF) spectra of the shortest pulses were recorded to verify the stability of the ML operation in different frequency span ranges, as shown in Fig. 7. The first beat note located at $\sim 70.8 \text{ MHz}$ exhibits a high extinction ratio of $>78 \text{ dBc}$ above carrier, see Fig. 7(a). The uniform harmonics on a 1-GHz frequency span revealed high stability of the single-pulse mode-locked operation without any Q-switching instabilities, see Fig. 7(b).

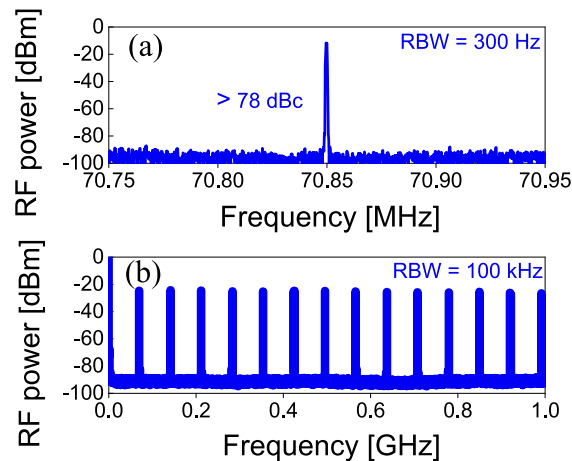


Fig. 7. RF spectra of the SESAM ML Yb:(Y,Gd)AlO₃ laser: (a) First beat note at ~70.8 MHz recorded with a resolution bandwidth (RBW) of 300 Hz, and (b) Harmonics on a 1-GHz frequency span recorded with a RBW of 100 kHz.

5. Conclusion

To conclude, the use of a “mixed” (solid-solution) composition of Yb:YAlO₃ crystals where a part of the Y³⁺ cations is replaced by Gd³⁺ ones improves the potential of orthoaluminate crystals for broadband wavelength tuning and ultrashort pulse generation at ~1 μm. In the present work, we achieved for the first time sub-50 fs pulses from a passively mode-locked Yb:(Y,Gd)AlO₃ laser representing the shortest pulse duration ever obtained using any Yb³⁺-doped orthoaluminate. By using a *c*-cut 5.65 at. % Yb:(Y,Gd)AlO₃ crystal, a single-transverse-mode fiber-coupled 976 nm InGaAs diode laser as a pump source, a commercial SESAM for initiating and stabilizing the mode-locked operation and a pair chirped mirrors for intracavity dispersion management, soliton pulses as short as 43 fs were generated at a central wavelength of 1052.3 nm corresponding to an average output power of 103 mW at a pulse repetition rate of ~70.8 MHz. Our laser results indicate the potential of “mixed” Yb:Y_{1-x}Gd_xAlO₃ crystals with optimized Y³⁺/Gd³⁺ ratios for further power scaling and pulse shortening via the Kerr-lens mode-locking technique [23–25].

Funding. National Natural Science Foundation of China (61975208, 61875199, 61905247, 51761135115, 61850410533, 62075090, 52032009, 51972149, 51872307, 61935010); Sino-German Scientist Cooperation and Exchanges Mobility Program (M-0040); the Science Foundation of Fujian Province (2019J02015); Key-Area Research and Development Program of Guangdong Province (2020B090922006).

Acknowledgment. Xavier Mateos acknowledges the Serra Hünter program.

Disclosures. The authors declare no conflicts of interest.

Data availability. Data underlying the results presented in this paper are not publicly available at this time but may be obtained from the authors upon reasonable request.

References

1. G. Boulon, Y. Guyot, H. Canibano, S. Hraiech, and A. Yoshikawa, “Characterization and comparison of Yb³⁺-doped YAlO₃ perovskite crystals (Yb:YAP) with Yb³⁺-doped Y₃Al₅O₁₂ garnet crystals (Yb:YAG) for laser application,” *J. Opt. Soc. Am. B* **25**(5), 884–896 (2008).
2. I. F. Elder and J. Payne, “Diode-pumped, room-temperature Tm:YAP laser,” *Appl. Opt.* **36**(33), 8606–8610 (1997).
3. P. Arsenov and K. Bienert, “Spectral properties of Ho³⁺ in GdAlO₃ crystals,” *Phys. Status Solidi A* **13**(2), K129–K132 (1972).
4. A. Rudenkov, V. Kisel, A. Yasukevich, K. Hovhannesian, A. Petrosyan, and N. Kuleshov, “Spectroscopy and continuous wave laser performance of Yb³⁺:LuAlO₃ crystal,” *Opt. Lett.* **41**(24), 5805–5808 (2016).
5. A. Rudenkov, V. Kisel, A. Yasukevich, K. Hovhannesian, A. Petrosyan, and N. Kuleshov, “Yb³⁺:LuAlO₃ crystal as a gain medium for efficient broadband chirped pulse regenerative amplification,” *Opt. Lett.* **42**(13), 2415–2418 (2017).

6. D. Li, Q. Liu, P. Zhang, H. Zhou, S. Zhu, Y. Zhang, Z. Li, H. Yin, Z. Chen, and Y. Hang, "Crystal growth, optical properties and laser performance of new mixed Nd³⁺ doped Gd_{0.1}Y_{0.9}AlO₃ crystal," *J. Alloys Compd.* **789**, 664–669 (2019).
7. R. Diehl and G. Brandt, "Crystal structure refinement of YAlO₃, a promising laser material," *Mater. Res. Bull.* **10**(2), 85–90 (1975).
8. V. E. Kisel, S. V. Kurilchik, A. S. Yasukevich, S. V. Grigoriev, S. A. Smirnova, and N. V. Kuleshov, "Spectroscopy and femtosecond laser performance of Yb³⁺:YAlO₃ crystal," *Opt. Lett.* **33**(19), 2194–2196 (2008).
9. L. Guillemot, P. Loiko, A. Braud, J.-L. Doualan, A. Hideur, M. Koselja, R. Moncorge, and P. Camy, "Continuous-wave Tm:YAlO₃ laser at ~2.3 μm," *Opt. Lett.* **44**(20), 5077–5080 (2019).
10. J. Tang, E. Li, F. Wang, W. Yao, C. Shen, and D. Shen, "High Power Ho:YAP Laser With 107 W of Output Power at 2117 nm," *IEEE Photonics J.* **12**(2), 1–7 (2020).
11. J. Petit, B. Viana, P. Goldner, J. P. Roger, and D. Fournier, "Thermomechanical properties of Yb³⁺ doped laser crystals: Experiments and modeling," *J. Appl. Phys.* **108**(12), 123108 (2010).
12. Y. Song, N. Zong, K. Liu, Z. Wang, X. Wang, Y. Bo, Q. Peng, and Z. Xu, "Temperature-dependent thermal and spectroscopic properties of Yb:YAlO₃ perovskite crystal for a cryogenically cooled near IR laser," *Opt. Mater. Express* **10**(7), 1522–1530 (2020).
13. R. Aggarwal, D. Ripin, J. Ochoa, and T. Fan, "Measurement of thermo-optic properties of Y₃Al₅O₁₂, Lu₃Al₅O₁₂, YAlO₃, LiYF₄, LiLuF₄, BaY₂F₈, KGd(WO₄)₂, and KY(WO₄)₂ laser crystals in the 80 - 300 K temperature range," *J. Appl. Phys.* **98**(10), 103514 (2005).
14. A. Rudenkov, V. Kisel, A. Yasukevich, K. Hovhannesian, A. Petrosyan, and N. Kuleshov, "High power SESAM mode-locked laser based on Yb³⁺:YAlO₃ bulk crystal," *Devices Methods Measure.* **11**(3), 179–186 (2020).
15. R. Akbari, P. Loiko, J. Xu, X. Xu, and A. Major, "Performance of diode-pumped Yb:YAP lasers with different crystal orientations," *Proc. SPIE* **11259**, 112591T (2020).
16. H. Zeng, H. Lin, Z. Lin, L. Zhang, Z. Lin, G. Zhang, V. Petrov, P. Loiko, X. Mateos, L. Wang, and W. Chen, "Diode-pumped sub-50-fs Kerr-lens mode-locked Yb:GdYCOB laser," *Opt. Express* **29**(9), 13496–13503 (2021).
17. T. Huiyu, W. Rui, Z. Peixiong, Y. Hao, L. Zhen, and C. Zhenqiang, "Growth and properties of Gd³⁺/Yb³⁺ co-doped yttrium aluminate crystals," *J. Synth. Cryst.* **50**(11), 2013–2018 (2021).
18. Y. Wang, X. Chen, P. Zhang, Z. Li, Y. Hang, E. Ji, H. Li, and Z. Chen, "Growth, spectroscopic features and efficient 2 μm continuous-wave laser output of a Tm³⁺:Gd_{0.1}Y_{0.9}AlO₃ disordered crystal," *Opt. Laser Technol.* **131**, 106421 (2020).
19. F. Druon, F. Balembois, and P. Georges, "New Materials for Short-Pulse Amplifiers," *IEEE Photonics J.* **3**(2), 268–273 (2011).
20. R. Gaumé, B. Viana, D. Vivien, J. P. Roger, and D. Fournier, "A simple model for the prediction of thermal conductivity in pure and doped insulating crystals," *Appl. Phys. Lett.* **83**(7), 1355–1357 (2003).
21. J. A. Caird, S. A. Payne, P. Staber, A. Ramponi, L. Chase, and W. F. Krupke, "Quantum electronic-properties of the Na₃Ga₂Li₃F₁₂:Cr³⁺ laser," *IEEE J. Quantum Electron.* **24**(6), 1077–1099 (1988).
22. Y. Zaouter, J. Didierjean, F. Balembois, G. L. Leclin, F. Druon, P. Georges, J. Petit, P. Goldner, and B. Viana, "47-fs diode-pumped Yb³⁺:CaGdAlO₄ laser," *Opt. Lett.* **31**(1), 119–121 (2006).
23. P. Sévillano, P. Georges, F. Druon, D. Descamps, and E. Cormier, "32-fs Kerr-lens mode-locked Yb:CaGdAlO₄ oscillator optically pumped by a bright fiber laser," *Opt. Lett.* **39**(20), 6001–6004 (2014).
24. S. Uemura and K. Torizuka, "Sub-40-fs Pulses from a Diode-Pumped Kerr-Lens Mode-Locked Yb-Doped Yttrium Aluminum Garnet Laser," *Jpn. J. Appl. Phys.* **50**(1), 010201 (2011).
25. Z. Gao, J. Zhu, J. Wang, Z. Wei, X. Xu, L. Zheng, L. Su, and J. Xu, "Generation of 33 fs pulses directly from a Kerr-lens mode-locked Yb:CaYAlO₄ laser," *Photonics Res.* **3**(6), 335–338 (2015).